BIOCHEMISTRY
including biophysical chemistry & molecular biology

Article

pubs.acs.org/biochemistry

The FKBP−Rapamycin Binding Domain of Human TOR Undergoes Strong Conformational Changes in the Presence of Membrane Mimetics with and without the Regulator Phosphatidic Acid

Diana C. Rodriguez Camargo,[†] Nina M. Link,[‡] and Sonja A. Dames*,[†]

[†]Biomolecular NMR Spectroscopy, Department of Chemistry, Technische Universität München, Munich, Germany

[‡]Biozentrum, University of Basel, Basel, Switzerland

Supporting Information

ABSTRACT: The Ser/Thr kinase target of rapamycin (TOR) is a central controller of cellular growth and metabolism. Misregulation of TOR signaling is involved in metabolic and neurological disorders and tumor formation. TOR can be inhibited by association of a complex of rapamycin and FKBP12 to the FKBP12−rapamycin binding (FRB) domain. This domain was further proposed to interact with phosphatidic acid (PA), a lipid second messenger present in cellular membranes. Because mammalian TOR has been localized at various cellular membranes and in the nucleus, the output of TOR signaling may depend on its localization, which is expected to be influenced by the interaction with complex partners and regulators in response to cellular signals. Here, we present a detailed characterization of the interaction of the FRB domain with PA and how it is influenced by the surrounding membrane environment. On the basis of nuclear magnetic resonance- and circular dichroism-monitored binding studies using different neutral and negatively charged lipids as well as different membrane mimetics (micelles, bicelles, and liposomes), the FRB domain may function as a conditional peripheral membrane protein. However, the data for the isolated domain just indicate an increased affinity for negatively charged lipids and membrane patches but no specific preference for PA or PA-enriched regions. The membrane-mimetic environment induces strong conformational changes that largely maintain the α-helical secondary structure content but presumably disperse the helices in the lipidic environment. Consistent with overlapping binding surfaces for different lipids and the FKBP12−rapamycin complex, binding of the inhibitor complex protects the FRB domain from interactions with membrane mimetics at lower lipid concentrations.

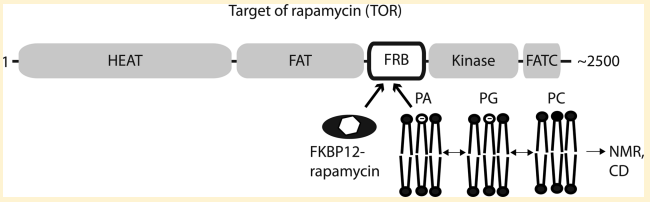

The Ser/Thr kinase target of rapamycin (TOR) is a central controller of cell growth and survival as well as cytoskeletonal reorganization processes in all eukaryotes.[1−3] TOR forms two distinct multiprotein complexes termed TORC1 and TORC2.[4] TORC1 controls the accumulation of cell mass in response to the nutrient and energy state of the cell, which is, for example, sensed through the presence of growth factors like insulin or the ATP:AMP ratio.[1,5] Processes controlled by TORC1 include protein and lipid synthesis, ribosome and mitochondrial biogenesis, and autophagy.[1,3,5] TORC2 influences cell survival and action cytoskeleton organization. Both TOR complexes intercept several signaling pathways,[6,7] and misregulation of these pathways is found in many types of metabolic and neurological disorders as well as cancer.[5,8−12] TOR has further been implicated in the immune response.[3] Whereas TORC1 is highly sensitive to the TOR-specific inhibitor complex composed of the macrolide rapamycin and the cellular protein FKPB12, TORC2 is affected by only long-term exposure to rapamycin.[4,13,14]

The highly conserved TOR proteins are ~2500 residues long and share several functional domains (Figure 1a).[2] The N-terminal HEAT repeat-rich region[15] and the following FAT domain,[16] which presumably is also composed of an α-helical repeat motif, have been suggested to mediate protein−protein interactions.[15,16] The FKBP12−rapamycin binding (FRB) domain is ~100 amino acids long and just N-terminal of the catalytic Ser/Thr kinase domain, which encompasses ~250−350 residues. The C-terminal FATC domain plays an important role in the regulation of TOR function[17] and has been suggested to influence the stability of TOR through its redox state[18] as well as to contribute to TOR membrane interactions.[19]

TOR has been localized at various cellular membranes (Golgi, ER, lysosomes, mitochondria, and plasma membrane)[20−25] and in the nucleus.[26] In addition, TOR was recently found to be associated with ribosomes.[27] On the basis of these observations, the output of TOR signaling was suggested to depend on its cellular localization,[20] which itself should be regulated by pathway-specific stimuli and the composition of each TOR complex. Earlier studies indicated that protein−protein interactions mediated by the HEAT repeat region play an important role in plasma membrane localization in yeast.[21] In addition, several proposed regulators

Received: February 16, 2012
Revised: April 26, 2012
Published: May 23, 2012

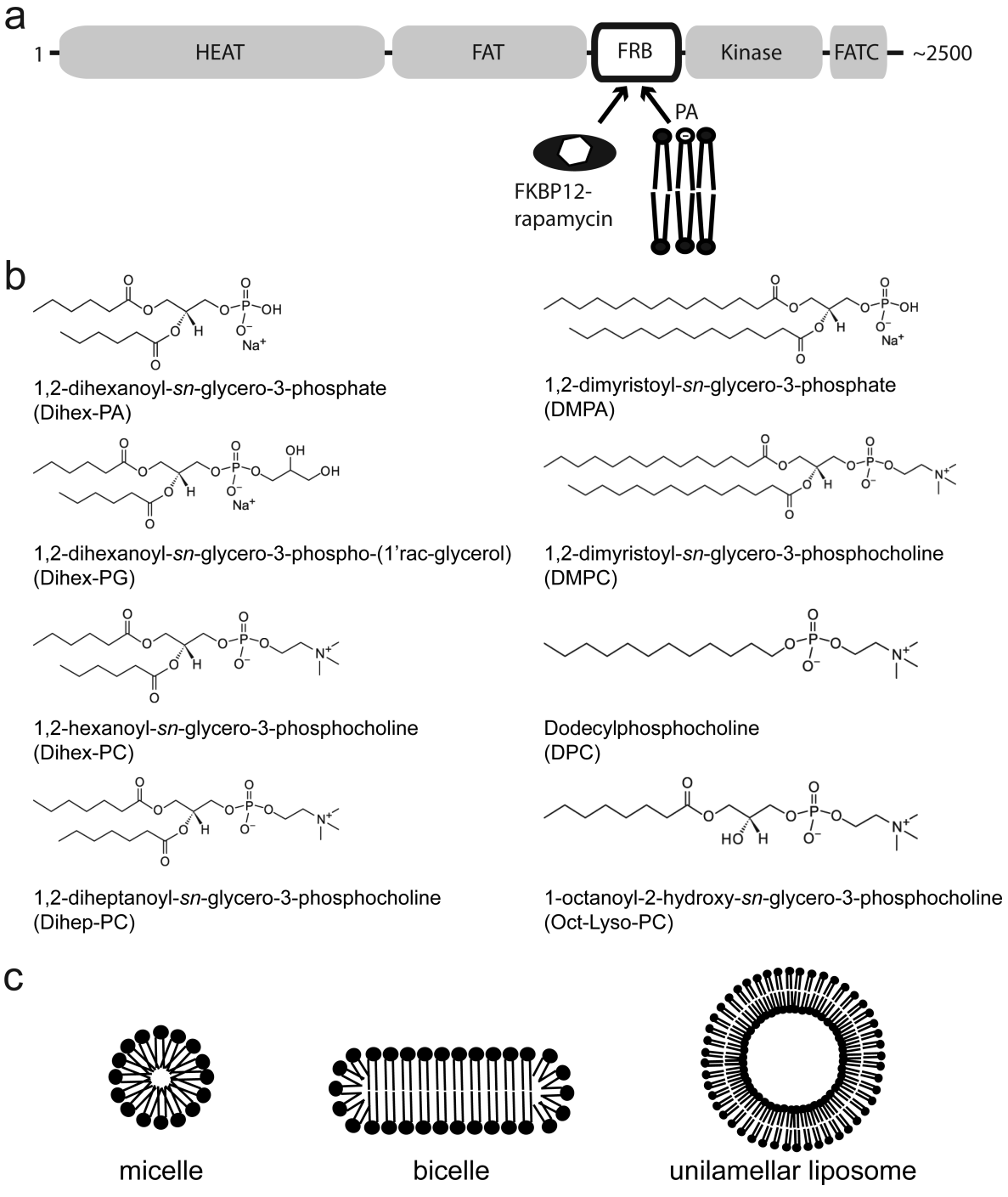

Figure 1. Domain structure of TOR proteins and schematic representations of lipids and membrane mimetics used in this study. (a) TOR proteins share several functional regions. The N-terminal ~1200-amino acid region is composed of HEAT repeats (huntingtin, elongation factor 3, regulatory subunit A of PP2A) and is followed by the ~550-residue FAT (FRAP, ATM, TTRAP) domain. The ~100-amino acid FKBP12−rapamycin binding (FRB) domain is to the N-terminal side of the ~250−350-amino acid Ser/Thr kinase domain. This domain was also suggested to interact with phosphatidic acid (PA), a phospholipid component of cellular membranes. At the C-terminus is the highly conserved, ~35-residue FATC (FAT C-terminal) domain. The FRB domain is overall also very conserved; an alignment of the amino acid sequences of this domain from different organisms is shown in Figure S2 of the Supporting Information. (b) Chemical structures of the lipids used in this study. For comparison, a PC lysolipid that is similar in length to DPC is also shown. The abbreviations used within the text are given. All lipid structure pictures were obtained from the website of Avanti Polar Lipids (http://avantilipids.com/). (c) Schematic representation of different membrane mimetics.

and interaction partners of TOR have membrane anchoring domains or fatty acid modifications, for example, the GTPases Rheb and Rac1 that are lipidated and thereby associate with endosomal membranes and the plasma membrane, respectively, or FKBP38 that has a transmembrane domain and thereby localizes to the mitochondrial membrane.[28−30] Besides this, direct TOR lipid and membrane interactions were suggested. On the basis of nuclear magnetic resonance (NMR) binding and structural studies with lipids with different headgroups and using different membrane mimetics such as micelles and

dx.doi.org/10.1021/bi3002133 | *Biochemistry* 2012, 51, 4909−4921

bicelles, the redox-sensitive FATC domain was suggested to contain a membrane anchor that consists of a hydrophobic bulb that has a rim of charged residues.[19] Moreover, the FRB domain has been shown to mediate interactions with the lipid second messenger phosphatidic acid (PA).[31] PA accounts for 1−4% of the total lipid content of cellular membranes.[32] Important with respect to TOR signaling is the generation of PA by phospholipases D1 and D2 (PLD1/2) and by the glycerol 3-phosphate pathway.[33−36] PLD2 is mainly localized at the plasma membrane, and its activity depends on the concentration of diacylphosphoinositol-4,5-bisphosphate (PIP45).[32,34] On the basis of later studies, PLD-generated PA is required for the association of TOR with Raptor to form TORC1 as well as with Rictor to form TORC2.[37] The effect of PA is competitive with rapamycin, with significantly higher concentrations needed to complete the interaction with TORC2 than with TORC1.[37] In contrast, PA generated by the glycerol 3-phosphate pathway was suggested to inhibit TORC2 by destabilizing the interaction with Rictor.[36] The inhibitory effect coincided thereby with increased levels of PA-containing palmitate (16:0) acyl chains.[36] NMR studies with a water-soluble PA variant with only C6 fatty acid tails (Dihex-PA) showed that PA induces specific chemical shift changes in a surface region of the FRB domain that is formed by the N-terminal half of α-helix 1 and the C-terminal half of α-helix 4.[38] Because cellular PA is embedded in a membrane environment, we present here a more detailed characterization of the interaction of the FRB domain from human TOR (hFRB) with different lipids (Figure 1b) and membrane mimetics (Figure 1c) determined by NMR and CD spectroscopy. Our studies indicate that different membranelike environments induce large conformational changes in the FRB domain that overall preserve the α-helical secondary structure content but appear to disrupt the tertiary structure. Moreover, the interaction with PA appears not to be highly specific because phosphoglycerol (PG) and phosphocholine (PC) lipids as well as dodecylphosphocholine (DPC) induce very similar chemical shift changes. However, on the basis of the decrease in the signal intensity, the affinity for negatively charged lipids appears to be higher than for neutral ones.

MATERIALS AND METHODS

Protein Expression and Purification. The region encoding the human TOR FRB domain (hFRB, residues 2014−2114) was expressed and purified as described previously.[39] To improve the long-term stability and solubility of the isolated FRB domain, a second construct was prepared by site-directed mutagenesis that was N-terminally truncated by five and C-terminally by two residues; this is termed hFRBs (residues 2019−2112 of human TOR). The borders for the second construct were designed on the basis of the structured region as observed in the crystal structure of the free FRB domain [Protein Data Bank (PDB) entry 1AUE]. Expression, inclusion body extraction, reversed-phase high-performance liquid chromatography purification, and refolding were conducted as described previously for hFRB.[39] The yeast FKBP12 analogue FPR1 was also expressed and purified as described previously.[39] On the basis of a comparison of the $^{1}H-^{15}N$ HSQC spectra of hFRB and hFRBs in the absence and presence of the FKBP12−rapamycin complex (Figure S1 of the Supporting Information), shortening of the construct did not significantly alter the three-dimensional structure or its ability to interact with the inhibitor complex.

Sample Preparation for NMR and CD Experiments. NMR samples contained ∼50−150 μM ^{15}N-labeled hFRB or hFRBs and where mentioned an equimolar amount of unlabeled FKBP12 and rapamycin in 20 mM Tris buffer (pH 8, 95% H_2O/5% D_2O) with 1 mM TCEP, 300 mM NaCl, and 0.02% NaN_3. CD samples contained 11−65 μM protein. Dodecylphosphocholine (DPC), 1,2-dihexanoyl-*sn*-glycero-3-phosphate (Dihex-PA), 1,2-dihexanoyl-*sn*-glycero-3-phospho-(1′-*rac*-glycerol) (Dihex-PG), and 1,2-diheptanoyl-*sn*-glycero-3-phosphocholine (Dihep-PC) were purchased from Avanti Polar Lipids. 1,2-Dihexanoyl-*sn*-glycero-3-phosphocholine (Dihex-PC) was purchased from Sigma. 1,2-Dimyristoyl-*sn*-glycero-3-phosphate (DMPA) and 1,2-dimyristoyl-*sn*-glycero-3-phosphocholine (DMPC) were obtained from Genzyme Pharmaceuticals, and deuterated DPC (d_{38}-DPC) was from Cambridge Isotopes.

In general, lipid stock solutions for the titrations were prepared as follows. A defined amount of lipid from a concentrated stock in organic solvent (mostly chloroform) was placed in a glass vial and dried under a stream of nitrogen gas. The dried lipid was then dissolved in buffer or a protein sample. Only Dihep-PC was weighed and directly dissolved in buffer. The concentration of the used lipid stocks ranged from 5 mM to 1 M. For protein samples with a defined lipid concentration, an appropriate amount of the respective lipid in organic solvent was placed in a glass vial and dried under nitrogen gas before the protein solution was added. The acquisition of one-dimensional (1D) ^{1}H NMR spectra for each titration point allowed us to follow the increase in the lipid concentration as well as the shift of the equilibrium from free to micellar lipid, because micelle formation results in a shift of several lipid signals. In the samples with high DPC concentrations, the presence of micelles was further confirmed by NMR diffusion measurements.

Bicelles were prepared by first drying an appropriate amount of the long chain phospholipids in organic solvent (DMPC or DMPA) under a stream of nitrogen gas in a glass vial. The dried lipid was first resuspended in a small amount of buffer (20 μL), followed by the addition of the short chain lipid (DihepPC) in buffer. After the bicelle mixture had been thoroughly vortexed, the protein solution was added.

Liposomes were prepared by drying an appropriate amount of DMPC in chloroform under a stream of nitrogen gas, followed by incubation under vacuum overnight to remove remaining traces of the organic solvent. The resulting pellet was dissolved in buffer to obtain a 100 mM solution. To resuspend the pellet, it was exposed to seven cycles of freezing in liquid nitrogen followed by incubation in a water bath at 40 °C and vortexing. To induce the formation of small unilamellar vesicles from large uni- and multilamellar vesicles, the DMPC suspension was incubated in a sonication bath for ∼0.5 h; during this time, the temperature increased from ∼20 to ∼50 °C. To remove the remaining large vesicles, the milky suspension was centrifuged in a tabletop centrifuge for 5 min at 14.8K rpm. This resulted in a clear supernatant and a rather big fluffy white precipitate. For the preparation of a sample of hFRBs in the presence of liposomes, we initially used only the supernatant that should contain small unilamellar vesicles (SUVs). Because the precipitate after centrifugation of the liposomes was very large and the lipid signal in the 1D ^{1}H spectrum of the respective sample was very small compared to the ones we usually observe for micelles and bicelles, we resuspended the liposome precipitate and added 50 μL of this

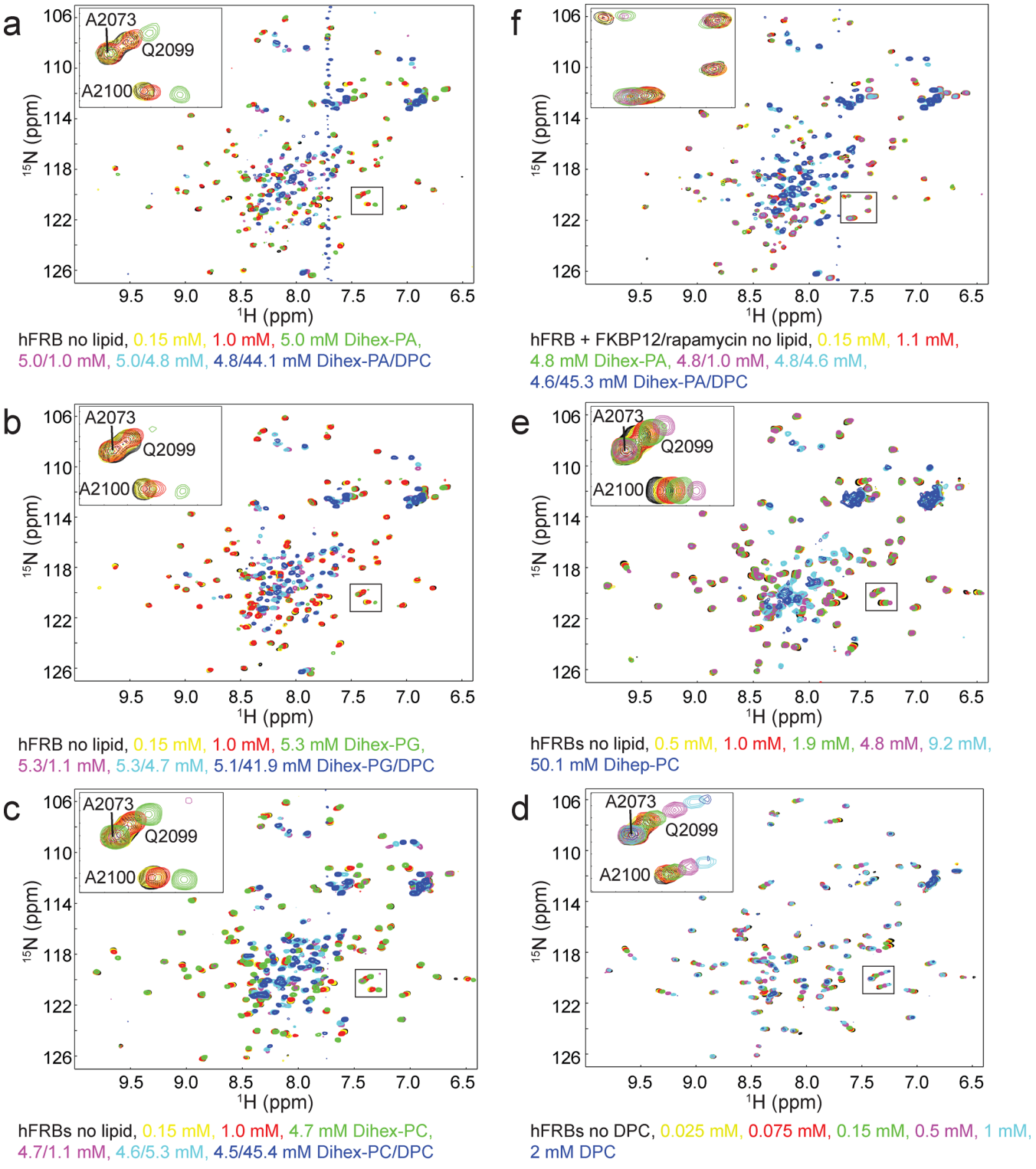

Figure 2. Interactions of the human TOR FRB domain with lipids and membrane mimetics as monitored by NMR spectroscopy. (a–f) $^{1}H-^{15}N$ HSQC spectra of [^{15}N]hFRB or [^{15}N]hFRBs in the presence of increasing amounts of lipids. The color coding of the spectra and the respective lipid concentrations are given below each plot. An enlarged view of the region highlighted with a black square is given in the top left corner of each spectrum.

more concentrated DMPC suspension to the 200 μL protein sample that had been prepared using 100 μL of the centrifuged liposome supernatant. However, the lipid signal remained rather small, presumably because of line broadening because of the huge size of the liposome particles.

NMR Spectroscopy. NMR spectra were recorded at 298 K on Bruker DRX600, DRX750, and DRX800 spectrometers. Titrations with different lipids were followed by recording regular or SOFAST[40] $^{1}H-^{15}N$ HSQC spectra. Data were processed with NMRPipe[41] and analyzed using NMRView.[42] The average chemical shift changes for the backbone amide

dx.doi.org/10.1021/bi3002133 | *Biochemistry* 2012, 51, 4909–4921

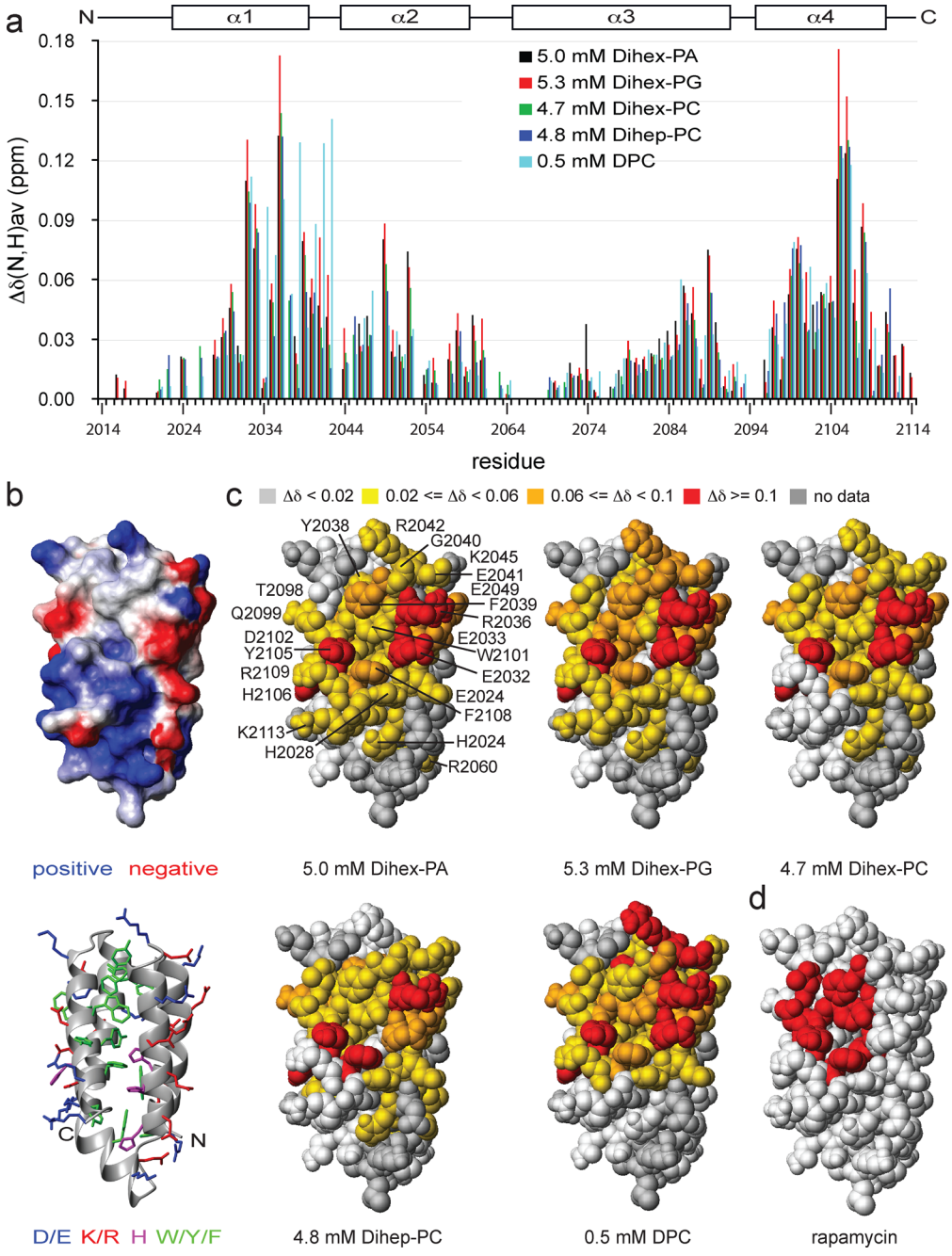

Figure 3. Analysis of the chemical shift changes observed for the human FRB domain at a concentration of ~5 mM for the indicated lipids and for 0.5 mM DPC. (a) Plot of the average chemical shift change for the backbone amide nitrogen and proton [$\Delta\delta$(N,H)av = $\Delta\delta$] as a function of the sequence position. The secondary structure elements are indicated at the top.[52] (b) The top picture shows a surface charge representation of the human FRB domain and the bottom picture a ribbon representation of the same structure. Positively charged surface areas or residues are colored blue and negatively charged ones red. For the bottom representation, the side chains of histidines were additionally colored magenta and those of tryptophans, tyrosines, and phenylalanines green. (c) For this representation, the chemical shift changes observed at a lipid concentration of ~5 mM for the indicated lipids and for 0.5 mM DPC (Figure 2a–e and panel a) have been mapped onto a space-filled model of the structure of the human FRB domain. Weak shifts are highlighted in yellow, medium shifts in orange, and strong shifts in red. For residues colored darker gray, no information could be obtained because of spectral overlap, missing signals, or unclear assignments. (d) For this surface representation of the FRB domain, the residues interacting with rapamycin in the crystal structure of a complex between the FRB domain and the FKBP12–rapamycin complex are colored red.[53] Representations of the structures in panels b–d corresponding to 180° rotations around the vertical axis are given in Figure S3 of the Supporting Information. All structures were made with MolMol[68] and POV-Ray (http://www.povray.org) using the crystal structure of the free FRB domain of human TOR (PDBentry 1AUE).[52]

nitrogen and proton [$\Delta\delta$(N,H)av] were calculated as $[(\Delta\delta_{HN})^2 + (\Delta\delta_N/5)^2]^{1/2}$. Chemical shift assignments for hFRB and hFRBs were adapted from the published values (BMRB entry 6760).[43] The lipid concentration during titration experiments varied in general from 0.05 to 50 mM; only in the titration with DPC alone did it range from 0.025 to 2 mM. NMR samples in the presence of micelles contained either 150 or 135 mM DPC and 15 mM DMPA. The lipid concentrations in the bicelle

dx.doi.org/10.1021/bi3002133 | Biochemistry 2012, 51, 4909–4921

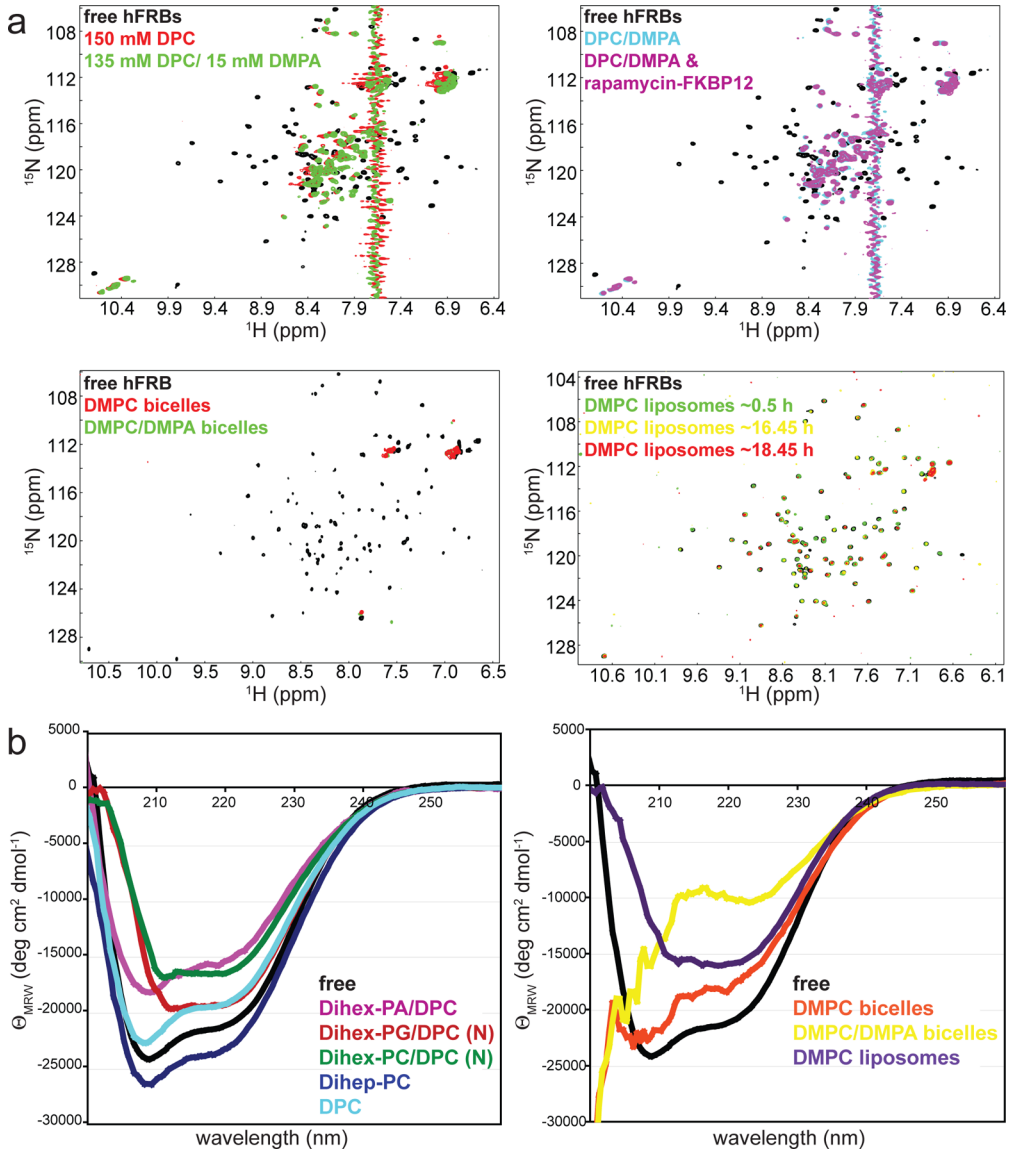

Figure 4. Influence of various membrane mimetics on the NMR spectra and secondary structure of the FRB domain of human TOR. (a) $^{1}H-^{15}N$ HSQC spectra of the free FRB domain in the presence of high concentrations of DPC or DPC/PA micelles (top left) and after addition of the unlabeled FKBP12−rapamycin complex at a 1:1 ratio with respect to the micelle-immersed FRB domain (top right). The bottom left representation shows $^{1}H-^{15}N$ HSQC spectra of the human FRB domain in the presence of DMPC or DMPC/DMPA bicelles (total lipid concentration of ~300 mM, 4:1 DMPC:DMPA ratio) and the bottom right picture spectra in the presence of DMPC liposomes (total lipid concentration of <60 mM) at different time steps. (b) The left plot shows CD spectra of the human FRB domain alone and in the presence of pure DPC micelles or such containing additionally the indicated diacyl lipid. (N) means that the spectrum was recorded using the more concentrated sample from the NMR titration. The DPC concentration was ~42−45 mM in the mixed micelles and 50 mM if DPC alone was used. The concentration of the diacyl lipid was ~5 mM. The right plot shows a superposition of the CD spectra of the free FRB domain and those in the presence of DMPC or DMPC/DMPA bicelles, or DMPC liposomes. Note that in the samples containing high protein concentrations and/or PC-based membrane mimetics the spectrum is distorted below ~220 nm because of an overly high voltage at the detector. See also Figure S4 of the Supporting Information and the text.

samples were 72 mM DMPC or 15 mM DMPA with 57 mM DMPC and 239 mM Dihep-PC, corresponding to a q of 0.3 and a c_L of 15%.

CD Spectroscopy. All CD spectra were recorded at room temperature on a Jasco J715 spectropolarimeter using a cuvette with a path length of 0.1 cm. All spectra were recorded with an acquisition time of 50 nm per minute (8 s response time) and five scans if not otherwise mentioned. The CD samples in the presence of micelles contained all ~50 mM lipid, either 50 mM DPC or ~5 mM Dihex-PA, Dihex-PG, or Dihex-PC, and ~45 mM DPC or 50 mM Dihep-PC. The lipid concentrations in the bicelle samples were 44.8 mM DMPC or 9.4 mM DMPA with 35.3 mM DMPC and 147.9 mM Dihep-PC, corresponding to a q of 0.3 and a c_L of 9.3%.

RESULTS

Different Lipids Induce Similar Spectral Changes in the TOR FRB Domain. Ververka et al. have shown that Dihex-PA, which because of its short acyl chains is well water-soluble, induces specific spectral changes in the FRB domain of TOR.[38] Because they had used a slightly different construct, which had an additional non-native N-terminal extension, we first tried to reproduce their observations with our nontagged construct. Increasing the Dihex-PA concentration from ~0 to 5 mM

dx.doi.org/10.1021/bi3002133 | Biochemistry 2012, 51, 4909−4921

induces specific chemical shift changes (Figure 2a). At ∼0.15 mM Dihex-PA (Figure 2a, yellow spectrum), there are no significant spectral changes. From 1 to 5 mM (Figure 2a, red and green spectra), many peaks shift gradually, which is accompanied by a decrease in intensity. The strength of the observed chemical shift changes at 5 mM Dihex-PA as a function of the sequence (Figure 3a) reproduces very well the data published by Ververka et al.[38] Also, in our case, the strongest chemical shift changes localize to residues on the surfaces of α-helices 1 and 4 (Figure 3c).

PA is a component of cellular membranes; therefore, the surrounding membrane environment is expected to influence the interaction with PA. Because Dihex-PA has a very high CMC (>10 mM) and negatively charged PA contributes only a fraction of the membrane lipids, a neutral membrane mimetic was added in increasing amounts to induce micelle formation. We used DPC, because it has a rather low CMC (1.1 mM)[44] and is a well-established membrane mimetic for solution NMR studies.[19,45−48] The presence of 1 mM DPC in addition to 5 mM Dihex-PA (Figure 2a, magenta spectrum), which is expected to induce the formation of micelles, results in a complete change in the spectrum. The resonances for the free form that had shifted only upon addition of 5 mM Dihex-PA disappear, and new resonances appear. Increasing the DPC concentration to 5 mM and subsequently to 44 mM (Figure 2a, cyan and blue spectra) increases the concentration of micelles and shifts the equilibrium to the micelle-immersed state. This results in an overall increase in the peak intensities of the bound form that is accompanied by additional small chemical shift changes. Using even higher concentrations of PA and DPC [15 mM DMPA and 135 mM DPC (Figure 4a, green spectrum)] shifts the equilibrium further to the micelle-immersed state, resulting in a further increase in the respective peak intensities. The spectrum of the micelle-immersed state is characterized by a narrow chemical shift dispersion. This indicates that the chemical environment of the residues became overall more uniform. Approximately 70 peaks can be counted for the backbone amide groups of the micelle-immersed state (Figure 4a, green spectrum). On the basis of the shape and intensity, several of them must correspond to more than one peak. The number of peaks in the region where the glycine backbone amide groups are typically visible (∼105−110 ppm) indicates that the spectrum of the micelle-associated form shows presumably most to all of the expected resonances (≤91 for hFRBs; 94 minus 2 Pro residues minus the N-terminal residue).

The specificity of the interaction of the FRB domain with PA was first evaluated from a titration of [^{15}N]hFRB with Dihex-PG that has as PA a negatively charged headgroup (Figure 1b). The titration was done exactly as with Dihex-PA. At first, the concentration of Dihex-PG was increased in small steps from 0 to ∼5 mM, and then DPC was added from a concentration of 1 to 42 mM to induce the formation of micelles (Figure 2b). The observed spectral changes with 5 mM Dihex-PG are highly similar to those with Dihex-PA, only that the chemical shift differences and the decrease in the peak intensities are slightly larger (Figures 2a,b and 3a). The NMR spectra in the additional presence of DPC are also highly similar for PA and PG (Figure 2a,b, dark blue spectra).

Because both lipids with negatively charged headgroups resulted in overall comparable chemical shift changes, we also titrated the FRB domain with the neutral lipid Dihex-PC (Figure 1b). Again, Dihex-PC was first added in small steps, from 0 to ∼5 mM, followed by addition of DPC from a concentration of 1 to 45 mM to induce the formation of micelles (Figure 2c). At ∼5 mM Dihex-PC, the pattern of chemical shift changes is overall similar to those observed for the two negatively charged lipids (Figure 3a); however, the signal intensity of the peaks is still considerably higher, indicating a lower affinity for the neutral phospholipid (Figure 2c, green spectrum). The formation of micelles due to addition of DPC results as for Dihex-PA and Dihex-PG in a complete change in the appearance of the spectra (Figure 2c, magenta, cyan, and blue spectra).

The influence of DPC in the absence of PA, PG, or PC at concentrations below or slightly above its CMC (1.1 mM)[44] was determined from a titration of hFRBs with 0−2 mM DPC (Figure 2d). Unexpectedly, the pattern of chemical shift changes in the presence of only 0.5 mM DPC is very similar to that for ∼5 mM Dihex-PA, Dihex-PG, or Dihex-PC (Figure 3a). Only several residues in the first α-helix show slightly stronger and some in the fourth α-helix slightly smaller chemical shift changes. DPC has as Dihex-PC a neutral phosphocholine headgroup (Figure 1b). This further indicates that the FRB domain appears not to interact only with lipids with a headgroup with a net negative charge. Compared to Dihex-PA, -PG, and -PC, DPC has only a single but longer fatty acid chain and thus more resembles a lysolipid (Figure 1b). This may at least in part explain why only 0.5 mM DPC induces chemical shift changes similar to those induced by the tested dihexanoyl phospholipids at ∼5 mM. The spectrum of the micelle-immersed state at high concentrations of pure DPC [150 mM (Figure 4a, red spectrum)] looks very similar to that obtained with DPC micelles containing additionally ∼10% Dihex-PA [15 mM Dihex-PA and 135 mM DPC (Figure 4a, green spectrum)].

The influence of the headgroup charge and the length and number of fatty acid chains was further derived from a titration of hFRBs with 0−50 mM Dihep-PC (Figure 2e). The pattern of the induced chemical shift changes at ∼4.8 mM is overall similar to those obtained for ∼5 mM Dihex-PA, Dihex-PG, or Dihex-PC as well as for 0.5 mM DPC (Figure 3a). However, the decrease in signal intensity at ∼5 mM (Figure 2e, magenta spectrum) is as for Dihex-PC (Figure 2c, green spectrum) lower than for the negatively charged lipids Dihex-PA and Dihex-PG (Figure 2a,b, green spectra). The CMC for Dihep-PC from the literature is ∼1.4−1.8 mM[49,50] and thereby only somewhat higher than that for DPC (1.1 mM).[44] Therefore, the difference in the length and/or number of fatty acid chains as well as the presence of the glycerol backbone between the phosphate group and the fatty acid chain in Dihep-PC (Figure 1b) may be responsible for the fact that lower concentrations of DPC versus those of Dihep-PC are necessary to achieve chemical shift changes similar in strength. At the next titration point (9.2 mM) at which the majority of Dihep-PC molecules are expected to be present in micelles, the appearance of the spectra changes completely (Figure 2e, cyan spectrum). The resulting spectrum looks overall similar to those obtained with 5 mM Dihex-PA, -PG, and -PC or 1−5 mM DPC (Figure 2a−c, magenta and cyan spectra). However, increasing the Dihep-PC concentration further to 50 mM appears to broaden the peaks of the micelle-immersed state (Figure 2e, dark blue spectrum). This observation can be explained by the fact that Dihep-PC micelles are very polydisperse and show a significant increase in micellar weight as the lipid concentration increases.[51] In summary, the titrations with different lipids indicate that the FRB domain shows a similar pattern of chemical shift changes

dx.doi.org/10.1021/bi3002133 | Biochemistry 2012, 51, 4909−4921

for all tested lipids (Figure 3a). However, the data indicate an increased affinity for negatively charged lipids and membrane regions compared to neutral ones. Besides the charge of the lipid headgroups, differences in the shape and packing of the respective formed micelles appear to influence the affinity for a specific membrane-mimetic structure.

Because DPC may just unspecifically destabilize the tertiary structure, we further analyzed the influence of DPC on a protein that was not suggested to interact with membranes. For this, we titrated the B1 domain of streptococcal protein G (GB1) with 0−50 mM DPC (Figure S5 of the Supporting Information). The respective $^{1}H-^{15}N$ HSQC spectra indeed show no significant spectral changes.

α-Helices 1 and 4 of the Four-Helix Bundle Exhibit the Strongest Lipid-Induced Chemical Shift Changes. A plot of the observed chemical shift changes for ∼5 mM Dihex-PA, Dihex-PG, Dihex-PC, or Dihep-PC or 0.5 mM DPC (Figure 3a) illustrates that the strongest chemical shift changes at lower lipid concentrations are observed in α-helices 1 and 4, which pack antiparallel with respect to each other in the four-helix bundle (Figure 3b). For Figure 3c, the chemical shift changes have been classified and mapped onto a surface representation of the crystal structure of the FRB domain (PDB entry 1AUE).[52] The residues showing medium to strong changes cluster to a hydrophobic surface region that is surrounded by several positively charged and some negatively charged residues. The two α-helices 1 and 4 forming this surface region contain several highly or completely conserved aromatic and aliphatic as well as charged residues (Figure S2 of the Supporting Information). Among these, E2032, E2033, R2036, A2100, Y2105, H2106, and F2108 show medium to strong backbone chemical shift changes in all five titrations using the free FRB domain (Figures 2a−e and 3a). E2032 and E2033 are in very few sequences replaced with aspartate. R2036, A2100, and F2108 are replaced with another residue in only one of the sequences from organisms having two TOR proteins such as yeast or silk moth. Position 2106 is in the sequences of higher eukaryotes always occupied by histidine; only some lower eukaryotes like yeast or *Dictyostelium* have asparagine or glutamate at this position or in the case of brown alga an aspartate. The sequence of TOR from brown alga is the least conserved compared to the other TOR sequences (Figure S2 of the Supporting Information). For Figure 3d, the residues that make interactions with rapamycin in the crystal structure of the ternary complex of the FRB domain with rapamycin and FKBP12 (PDB entry 1FAP)[53] are colored red. A comparison of the binding region for rapamycin (Figure 3d) with those for the tested lipids (Figure 3c) indicates that they strongly overlap.

Bicelles and Liposomes Also Induce Changes in the NMR Spectra of the FRB Domain. The membrane association of conditional peripheral membrane proteins depends not only on the surface charge but also on other factors such as curvature or lipid packing.[54] Because micelles are rather small spherical particles with a high curvature (Figure 1c, left), the interaction with more planar bicelles (Figure 1c, middle) was also tested. Figure 4a shows a superposition of the spectra of the FRB domain in the free form and in the presence of neutral DMPC and negatively charged DMPC/DMPA bicelles. The rim was always formed by Dihep-PC. In both cases, the interaction with the large bicelles (>250 kDa) resulted in the disappearance of nearly all backbone resonances, presumably because of broadening of the respective NMR signals beyond detection. On the basis of these data, the interaction of the FRB domain with membrane mimetics appears not to be very sensitive to the different surface properties of bicelles versus micelles.

Fang et al. suggested that the FRB domain mediates the regulation of TOR by PA because the isolated FRB domain bound strongly to liposomes containing a significant amount of PA (from 50 to 10%) but apparently not to neutral liposomes consisting of only PC.[31] Fang et al. incubated ∼18 μM purified FRB domain with ∼5 mM lipid, forming the respective liposome, and then applied the mixture to a gel filtration column to separate free protein from liposome-bound and free liposomes, the latter two both eluting in the void volume. The amount of protein in each fraction was determined by sodium dodecyl sulfate−polyacrylamide gel electrophoresis analysis.[31] Because we observed small chemical shift changes already with 5 mM Dihex-PC indicating a weak interaction as well as a complete spectral rearrangement in the presence of neutral micelles and bicelles, we wondered if the interaction of the FRB domain with neutral liposomes (Figure 1c, right) may have been too weak to be detected by the experimental setup used by Fang et al.[31] The $^{1}H-^{15}N$ HSQC spectrum of the FRB domain recorded shortly after it had been mixed with an aqueous suspension of liposomes shows no strong chemical shift changes of single peaks (Figure 4a, bottom right). However, in the spectrum recorded after incubation overnight, several peaks are weaker or had disappeared, which was even more pronounced in the spectrum recorded 2 h later. After the sample had been ejected from the NMR machine, it exhibited a fluffy precipitate. On the basis of the UV-determined protein concentration and CD spectra of the supernatant (see below) and the resuspended pellet, the precipitate consisted mostly of lipid, presumably large uni- and multilamellar lipid vesicles that had been present in the liposome preparation. It should be noted that because of the used preparation procedure and the properties of the resulting liposomes (size and formation of vesicles consisting of single as well as multiple bilayers) the amount of solvent accessible membrane surface using, for example, 100 mM lipid is much smaller compared to that of micelles and bicelles prepared using the same amount of lipid. This and the fact that the lipid concentration in the liposome sample was less than 60 mM may at least in part explain why the observed spectral changes occurred more slowly and less drastically than for bicelles and why Fang et al. did not observe an interaction with ∼5 mM neutral PC liposomes.[31] It should also be noted that in our bicelle NMR samples the total lipid concentration was ∼300 mM and therefore presumably sufficiently high to drive the equilibrium to the bicelle-associated state.

Membrane Mimetics Can Disrupt the Interaction with the FKPB12−Rapamycin Inhibitor Complex. Because the FKPB12−rapamycin inhibitor complex has been suggested to compete with PA for binding to the FRB domain and because the binding regions for both overlap (Figure 3c,d), we further analyzed how formation of a complex with the FKBP12−rapamycin species influences the interaction with PA and DPC. First, [^{15}N]hFRB in a complex with the unlabeled FKPB12−rapamycin species was titrated with Dihex-PA and DPC (Figure 2f) exactly as the free FRB domain (Figure 2a). As in the titration of the free FRB domain, up to ∼5 mM PA several peaks shift. However, the decrease in signal intensity is generally lower than for the free form. Moreover, the additional presence of 1 mM DPC only further weakens or shifts several peaks but does not yet induce a complete change in the

spectrum as observed for the free FRB domain. The latter is observed only at the next titration point (~5 mM Dihex-PA and ~5 mM DPC). This suggests that binding of the inhibitor complex (K_d = 12 nM)[55] can, at least in part, protect the FRB domain from lipid/membrane-induced conformational changes at lower lipid concentrations (lower than ~10 mM). The shift of peaks up to 5 mM indicates that PA can already interact with FKBP12−rapamycin complex-associated hFRB below the CMC. The final spectrum of the micelle-immersed form at higher lipid concentrations (4.6 mM Dihex-PA and 45.3 mM DPC) looks overall like that obtained for the free FRB domain (Figure 2a,f, dark blue spectra). Second, a mixture of FKBP12 and rapamycin was added in a 1:1 ratio to [^{15}N]hFRBs that had been immersed in a large amount of micelles composed of DPC and DMPA (Figure 4a, top right). However, the spectrum did not significantly change, suggesting that in the presence of 135 mM DPC and 15 mM DMPA the inhibitor complex cannot recognize the micelle-immersed state and/or induce conformational changes that allow an interaction.

The Micelle-Immersed State Shows an α-Helical Secondary Structure Content Similar to That of the Free Form. The ^{1}H−^{15}N HSQC spectra of the TOR FRB domain in the presence of high concentrations of membrane mimetics (Figure 2, blue spectra, and Figure 4a, top) show a narrow chemical shift dispersion. A very similar spectral appearance is usually observed for unstructured proteins, because unfolding of the protein chain results in a similar chemical environment for most residues and thereby in similar chemical shifts. To obtain information about the structure of the FRB domain in the presence of different membrane mimetics, CD spectra were recorded. For all membrane mimetics, a reference spectrum was recorded in buffer (Figure S4b of the Supporting Information) and used to correct the protein spectrum recorded in the presence of the respective membrane mimetic. This was particularly important for Dihep-PC/DMPC/DMPA bicelles, for DMPC liposomes, and for Dihep-PC micelles because all give a large to very large positive CD signal (Figure S4b of the Supporting Information). Therefore, CD spectroscopy may also be used to check and compare preparations of PC-based micelles, bicelles, or liposomes.

The CD spectrum of the free FRB domain (Figure 4b, black curve) is characteristic of a fully α-helical protein, in this case a four-helix bundle (Figure 3b). The CD spectra with neutral or negatively charged membrane-mimetic DPC-based micelles (Figure 4b, left plot) look very similar with respect to their shape. The shapes of the CD spectra in the presence Dihex-PG and DPC or Dihex-PC and DPC look different only below ~215 nm because for these measurements the significantly more concentrated NMR samples were used. The CD-monitored titration of hFRBs with DPC (Figure S4a of the Supporting Information) shows that the shape of the CD spectrum also does not change significantly if the DPC concentration is increased stepwise as during the NMR titration. The CD spectra in the presence of DMPC liposomes as well as DMPC- or DMPC/DMPA-based bicelles show a shape typical for an α-helical protein (Figure 4b, right plot). However, although the protein concentration was low, the spectra are significantly distorted below ~220 nm. This is because the respective membrane mimetics produce themselves a strong CD signal (Figure S4b of the Supporting Information), which together with the protein signal results in an overly high voltage of the detector. Altogether, the CD data indicate that the FRB domain in the presence of membrane mimetics maintains an overall content of α-helical secondary structure similar to that of the free form and that the interaction with membrane mimetics may only disrupt the tertiary structure and disperse the α-helices in the interior or on the surface of the micelle, bicelle, or liposome.

DISCUSSION

PA is the phospholipid component of cellular membranes with the smallest headgroup [-H (Figure 1b)]. Therefore, its headgroup is not expected to be as accessible on the membrane surface as, for example, the large headgroups of phosphoglycerol (Figure 1b) or phosphoinositides. Consistent with this, our studies with different membrane mimetics indicate that the surrounding membrane environment has a strong influence on the interaction of the FRB domain with PA. Moreover, higher concentrations of neutral membrane mimetics such as Dihep-PC (Figure 2e) or DPC micelles or Dihep-PC/DMPC bicelles (Figure 4a, left two plots) induced a complete change in the NMR spectrum even in the absence of PA. Such strong spectral changes in the presence of membrane mimetics were also observed for other known or putative conditional peripheral membrane proteins. A similar abrupt change in the ^{1}H−^{15}N HSQC spectrum that is characterized by a significant reduction in the extent of peak dispersion was, for example, observed for the anti-apoptotic protein Bcl-x_L[47,56] and for the putative GTPase-binding domain of *Dictyostelium* Formin C.[48] On the basis of additional CD and NMR data, Bcl-x_L maintains as the FRB domain a largely α-helical structure in the micelle-dissolved state,[47] whereas induction of additional α-helical secondary structure was proposed for Formin C.[48] Further studies revealed that key regulatory interactions of Bcl-2 family members occur at and in intracellular membranes (reviewed in ref 57), and the actin-binding protein Formin C was suggested to play a role in phagocytosis, which is regulated by GTPases and phosphoinositides.[58] Transformation of a β-strand into an α-helix and additional changes in the secondary and tertiary structure in the presence of micelles containing phosphoinositol 4,5-phosphate have further been reported for another actin-binding protein, gelsolin.[59]

Whereas the NMR titration data (Figure 2) indicate that the interaction with membrane-mimetic structures induces a rearrangement of the tertiary structure, it also shows that the FRB domain can interact with lipids below the CMC and therefore at concentrations at which no membrane-mimetic structures should be present. On the basis of the analysis of the observed chemical shift changes with Dihex-PA, -PG, and -PC up to ~5 mM (Figure 3a), thus ~5 mM below the CMC, the lipids can bind to a hydrophobic surface patch that overlaps with the binding region for the FKBP12−rapamycin complex (Figure 3c,d). In contrast to membrane mimetics, the interaction with single lipid molecules results in only small spectral and therefore conformational changes that overall maintain the fold. Thus, with the shift from low to high lipid concentrations, several association reactions occur: the interaction of the FRB domain with free lipids at low lipid concentrations and the association of lipid and DPC molecules to form micelles as well as the association of the FRB domain with micelles at lipid concentrations above the CMC.

Because neutral liposomes corresponding to a DMPC concentration of <60 mM resulted in NMR spectral changes significantly weaker than those seen with Dihep-PC/DMPC bicelles at a total lipid concentration of ~300 mM or Dihep-PC

micelles at a concentration of ≥10 mM, a strong interaction with a neutral membrane surface appears to happen in the presence of only a certain amount of solvent accessible membrane surface area. Because the FRB domain can also interact with single lipid molecules, the equilibrium between the free and the membrane-mimetic state in a micelle, bicelle, or liposome preparation may further play a role. In addition to the presence of negatively charged lipids, the membrane curvature, fluidity, and acyl chain accessibility may influence the affinity for membrane structures and thereby membrane-induced conformational changes.

Dihex-PA and the other tested lipids target a surface region on the FRB domain that overlaps with the binding region for rapamycin. In agreement with this, binding of the FKPB12−rapamycin complex protects the FRB domain at lower lipid concentrations from interacting with membrane mimetics. The fact that the binding sites for the FKPB12−rapamycin complex, PA, and other lipids overlap might in part explain why some mutations of the FRB domain affect the phosphorylation of target proteins in the absence of rapamycin or if they have no effect on the inhibition by rapamycin.[60] Some of these mutations may affect the interaction of either TOR complex with specific membrane patches and thereby influence substrate recognition. However, some mutations, especially of residues in the hydrophobic core, may also just destabilize the fold of the FRB (e.g., W2027F) and thereby hamper TOR function.

Fang et al.[31] described that mutating R2109 to alanine decreased the affinity for PA. Like Ververka et al.,[38] we observed only weak chemical shift changes for the backbone amide of R2109. However, Ververka et al. mentioned that they had observed significant shifts for the side chain amide of R2109.[38] Because the side chain of R2109 is located between two strongly shifting residues (Y2105 and H2106) (Figure 3c), it makes sense that it is affected by the interaction with PA and other lipids. The position corresponding to R2109 is in most TOR sequences (Figure S2 of the Supporting Information) occupied by an arginine; some have a lysine, and only one (fruit fly) has a glutamine. However, all sequences have additionally a positively charged residue at the neighboring position, R2110 in human TOR (Figure S2 of the Supporting Information), which may also participate in electrostatic interactions with negatively charged areas of lipid headgroups. In the titrations with PA and PG but also PC, the backbone amide of this residue shows a weak shift (Figure 3a). To the best of our knowledge, the effect of mutating R2110 on TOR signaling has not yet been studied.

The chemical shift changes for the two negatively charged lipids Dihex-PA and Dihex-PG at a concentration of ∼5 mM are nearly identical (Figures 2a,b and 3a). Initial studies using the isolated purified FRB domain and liposomes composed of PC alone or a mixture of 50% PC and 50% PA, PE, PI, or PS indicated that the FRB domain interacts strongly only with liposomes containing PA. On the basis of the small strip of the SDS gel documenting the amount of liposome-associated FRB, at least a small fraction appears to have bound to liposomes containing PS and, as far as what is visible, also to liposomes containing PI. Binding to liposomes containing PG was not tested. This raises the question of whether the FRB domain alone can be responsible for the specific effect of PA on TOR signaling or if other components of the TOR complex are involved. In addition, other negatively charged lipids or membrane-localized proteins could contribute to this effect. Whereas PLD-generated PA is needed for the interaction of TOR with Raptor in TORC1 and Rictor in TORC2,[37] PA generated in the glycerol 3-phosphate pathway inhibits TORC2 by destabilizing the TOR−Rictor interaction.[36] This discrepancy was explained by structural differences between the PA species generated in both pathways, with the inhibitory effect on TORC2 being specifically achieved by PA species containing palmitate (16:0) acyl chains.[36] Because TORC2 complexes can be further distinguished on the basis of the association with different isoforms of Sin1,[61] this may additionally influence the interaction with PA. Therefore, Raptor in TORC1 and Rictor/Sin1 in TORC2 may further influence or mediate the interaction with PA-containing membrane patches. This would also be consistent with the idea that TORC2 containing Rictor is sensitive to only a long-term exposure with rapamycin, because TORC2 has a higher affinity for PLD-generated PA than TORC1.[34]

As mentioned in the preceding paragraph, the inhibitory effect of PA on TORC2 was suggested to depend on its acyl chains.[36] In addition, DPC that resembles more a lysolipid (Figure 1b) induced below the CMC chemical shift changes in the FRB domain comparable to those induced by Dihex-PA. Therefore, the interaction of either TOR complex with PA-containing membrane patches may also depend on the local membrane composition and structure and the resulting accessibility of specific lipid acyl chains. Lysolipids are known to strongly influence the local membrane structure.[62] Thus, it may be possible that LPA influences TOR signaling not only indirectly by being the precursor for the synthesis of PA in the glycerol 3-phosphate pathway[36] or by stimulating PLD1 to produce PA[63] but also by directly influencing TOR−membrane association. Alternatively, another lysolipid could influence the local membrane structure and thereby increase the membrane affinity of the TOR FRB domain. Moreover, the interaction with PA-containing membrane patches may additionally depend on the interaction with membrane-associated regulators of PA-influenced TOR signaling such as phospholipase D2 (PLD2) that produces PA and has been shown to form a complex with TOR and Raptor[33] or the GTPases RalA and Arf6.[64]

Recently, it was shown that glucose starvation decreases the intracellular pH in yeast from ∼7−7.5 to ∼6.[65,66] This influences the interaction of the transcription factor Opi1 with PA, because it has a lower affinity for the protonated phosphate headgroup.[65] Because starvation also influences TOR signaling, its interaction with PA-containing membrane patches may also be pH-sensitive. In this respect, it is interesting to note that the determined lipid-binding surface of the FRB domain contains three histidines, H2024 and H2028 on α-helix 1 and H2106 on α-helix 4 (Figure 3b,c). The three histidines are conserved in all higher eukaryotes, whereas some lower eukaryotes have only one or two of them; only *Dictyostelium* has none. Using the crystal structure of the FRB domain of human TOR (PDB entry 1AUE) as input for PROPKA version 3.1,[67] the pK_a values for these three histidines were predicted to be in the range from ∼5.7 to ∼7 (5.98 and 6.92 for H2024, 6.06 and 6.69 for H2028, and 5.65 and 6.02 for H2106 for monomers A and B, respectively, of the crystal structure). Thus, lowering the pH below 6−7 could change the protonation state and thereby the affinity for negatively charged membrane patches. In mammalian cells, efficient glycolysis was thought to promote high cytosolic pH values; thus, glucose starvation may as in yeast result in a decrease in the cytosolic pH.[66]

In summary, our studies with different lipids and membrane mimetics suggest that the TOR FRB domain may function as a conditional peripheral membrane protein. However, the data for the isolated domain indicate not a strict specificity for PA or PA-containing membranes but simply an increased affinity for negatively charged lipids and surface patches. Specific differences of the membrane-immersed states in the presence or absence of PA or another negatively charged lipid have to be derived on the basis of the structure determination of the FRB domain in suitable membrane mimetics. Because the specific output of TOR signaling was suggested to depend on its subcellular localization, the latter is presumably regulated by a tight network of different interactions with complex partners and regulators as well as specific membrane regions. Future studies must therefore also target the structural and biophysical characterization of the interaction of TOR with other membrane components and membrane-associated regulatory proteins.

■ ASSOCIATED CONTENT

Supporting Information

Superpositions of the $^{1}H-^{15}N$ HSQC spectra of the used constructs of the FRB domain of human TOR in the presence and absence of the FKPB12−rapamycin inhibitor complex (Figure S1), an alignment of the amino acid sequences of the TOR FRB domain from different organisms (Figure S2), complementary views of the surface representations in Figure 3b−d (Figure S3), CD spectra of the titration of the TOR FRB domain with DPC and of the buffers and membrane mimetics (Figure S4), and a superposition of the $^{1}H-^{15}N$ HSQC spectra of the B1 domain of protein G in the presence of increasing amounts of DPC (Figure S5). This material is available free of charge via the Internet at http://pubs.acs.org.

■ AUTHOR INFORMATION

Corresponding Author

*Technische Universität München, Department of Chemistry, Biomolecular NMR Spectroscopy, Lichtenbergstr. 4, 85747 Garching, Germany. Phone: +49-(0)89-28913292. Fax: +49-(0)89-28913869. E-mail: sonja.dames@tum.de.

Funding

This work was supported from the German Research Foundation (DFG Grant DA1195/3-1) to S.A.D. N.L.M. was supported by a stipend from the Novartis foundation (Basel, Switzerland) and funding from the Freie Akademische Gesellschaft Basel (Basel, Switzerland).

Notes

The authors declare no competing financial interest.

■ ACKNOWLEDGMENTS

We thank Andrea Löschmann-Hage in Prof. Michael Hall's group at the Biozentrum of the University of Basel for help with the cloning and Prof. Hall for providing a template plasmid encoding full-length human TOR as well as an expression plasmid for yeast FKBP12. We acknowledge Klara Rathgeb-Szabo in Prof. Stephan Grzesiek's group for help during the purification of hFRB. We thank Prof. Stephan Grzesiek from the Biozentrum of the University of Basel for providing measurement time at his 800 MHz spectrometer for the acquisition of spectra in the presence of bicelles.

■ ABBREVIATIONS

Dihex-PA, 1,2-dihexanoyl-*sn*-glycero-3-phosphate; Dihep-PC, 1,2-diheptanoyl-*sn*-glycero-3-phosphocholine; Dihex-PC, 1,2-hexanoyl-*sn*-glycero-3-phosphocholine; Dihex-PG, 1,2-dihexanoyl-*sn*-glycero-3-phospho-(1′-*rac*-glycerol); DMPA, 1,2-dimyristoyl-*sn*-glycero-3-phosphate; DMPC, 1,2-dimyristoyl-*sn*-glycero-3-phosphocholine; DPC, dodecylphosphocholine; FKBP12, FK506 binding protein of 12 kDa, here equivalent to *Saccharomyces cerevisiae* FPR1; FRB, FKBP12−rapamycin binding; hFRB, residues 2014−2114 of human TOR; hFRBs, residues 2019−2112 of human TOR; (m)TOR, (mammalian) target or rapamycin.

■ REFERENCES

(1) Wullschleger, S., Loewith, R., and Hall, M. N. (2006) TOR signaling in growth and metabolism. *Cell 124*, 471−484.

(2) Jacinto, E., and Hall, M. N. (2003) Tor signalling in bugs, brain and brawn. *Nat. Rev. Mol. Cell Biol. 4*, 117−126.

(3) Araki, K., Ellebedy, A. H., and Ahmed, R. (2011) TOR in the immune system. *Curr. Opin. Cell Biol. 23*, 707−715.

(4) Loewith, R., Jacinto, E., Wullschleger, S., Lorberg, A., Crespo, J. L., Bonenfant, D., Oppliger, W., Jenoe, P., and Hall, M. N. (2002) Two TOR complexes, only one of which is rapamycin sensitive, have distinct roles in cell growth control. *Mol. Cell 10*, 457−468.

(5) Dazert, E., and Hall, M. N. (2011) mTOR signaling in disease. *Curr. Opin. Cell Biol. 23*, 744−755.

(6) De Virgilio, C., and Loewith, R. (2006) Cell growth control: Little eukaryotes make big contributions. *Oncogene 25*, 6392−6415.

(7) Corradetti, M. N., and Guan, K. L. (2006) Upstream of the mammalian target of rapamycin: Do all roads pass through mTOR? *Oncogene 25*, 6347−6360.

(8) Guertin, D. A., and Sabatini, D. M. (2007) Defining the role of mTOR in cancer. *Cancer Cell 12*, 9−22.

(9) Guertin, D. A., and Sabatini, D. M. (2005) An expanding role for mTOR in cancer. *Trends Mol. Med. 11*, 353−361.

(10) Tee, A. R., and Blenis, J. (2005) mTOR, translational control and human disease. *Semin. Cell Dev. Biol. 16*, 29−37.

(11) Choo, A. Y., and Blenis, J. (2006) TORgeting oncogene addiction for cancer therapy. *Cancer Cell 9*, 77−79.

(12) Bjornsti, M. A., and Houghton, P. J. (2004) The TOR pathway: A target for cancer therapy. *Nat. Rev. Cancer 4*, 335−348.

(13) Jacinto, E., Loewith, R., Schmidt, A., Lin, S., Ruegg, M. A., Hall, A., and Hall, M. N. (2004) Mammalian TOR complex 2 controls the actin cytoskeleton and is rapamycin insensitive. *Nat. Cell Biol. 6*, 1122−1128.

(14) Sarbassov, D. D., Ali, S. M., Sengupta, S., Sheen, J. H., Hsu, P. P., Bagley, A. F., Markhard, A. L., and Sabatini, D. M. (2006) Prolonged rapamycin treatment inhibits mTORC2 assembly and Akt/PKB. *Mol. Cell 22*, 159−168.

(15) Andrade, M. A., and Bork, P. (1995) HEAT repeats in the Huntington's disease protein. *Nat. Genet. 11*, 115−116.

(16) Bosotti, R., Isacchi, A., and Sonnhammer, E. L. (2000) FAT: A novel domain in PIK-related kinases. *Trends Biochem. Sci. 25*, 225−227.

(17) Takahashi, T., Hara, K., Inoue, H., Kawa, Y., Tokunaga, C., Hidayat, S., Yoshino, K., Kuroda, Y., and Yonezawa, K. (2000) Carboxyl-terminal region conserved among phosphoinositide-kinase-related kinases is indispensable for mTOR function in vivo and in vitro. *Genes Cells 5*, 765−775.

(18) Dames, S. A., Mulet, J. M., Rathgeb-Szabo, K., Hall, M. N., and Grzesiek, S. (2005) The solution structure of the FATC domain of the protein kinase target of rapamycin suggests a role for redox-dependent structural and cellular stability. *J. Biol. Chem. 280*, 20558−20564.

(19) Dames, S. A. (2010) Structural basis for the association of the redox-sensitive target of rapamycin FATC domain with membrane-mimetic micelles. *J. Biol. Chem. 285*, 7766−7775.

(20) Drenan, R. M., Liu, X., Bertram, P. G., and Zheng, X. F. (2004) FKBP12-rapamycin-associated protein or mammalian target of

rapamycin (FRAP/mTOR) localization in the endoplasmic reticulum and the Golgi apparatus. *J. Biol. Chem. 279*, 772−778.
(21) Kunz, J., Schneider, U., Howald, I., Schmidt, A., and Hall, M. N. (2000) HEAT repeats mediate plasma membrane localization of Tor2p in yeast. *J. Biol. Chem. 275*, 37011−37020.
(22) Wedaman, K. P., Reinke, A., Anderson, S., Yates, J., III, McCaffery, J. M., and Powers, T. (2003) Tor kinases are in distinct membrane-associated protein complexes in *Saccharomyces cerevisiae*. *Mol. Biol. Cell 14*, 1204−1220.
(23) Berchtold, D., and Walther, T. C. (2009) TORC2 plasma membrane localization is essential for cell viability and restricted to a distinct domain. *Mol. Biol. Cell 20*, 1565−1575.
(24) Withers, D. J., Ouwens, D. M., Nave, B. T., van der Zon, G. C., Alarcon, C. M., Cardenas, M. E., Heitman, J., Maassen, J. A., and Shepherd, P. R. (1997) Expression, enzyme activity, and subcellular localization of mammalian target of rapamycin in insulin-responsive cells. *Biochem. Biophys. Res. Commun. 241*, 704−709.
(25) Sancak, Y., Bar-Peled, L., Zoncu, R., Markhard, A. L., Nada, S., and Sabatini, D. M. (2010) Ragulator-Rag complex targets mTORC1 to the lysosomal surface and is necessary for its activation by amino acids. *Cell 141*, 290−303.
(26) Zhang, X., Shu, L., Hosoi, H., Murti, K. G., and Houghton, P. J. (2002) Predominant nuclear localization of mammalian target of rapamycin in normal and malignant cells in culture. *J. Biol. Chem. 277*, 28127−28134.
(27) Zinzalla, V., Stracka, D., Oppliger, W., and Hall, M. N. (2011) Activation of mTORC2 by association with the ribosome. *Cell 144*, 757−768.
(28) Saci, A., Cantley, L. C., and Carpenter, C. L. (2011) Rac1 regulates the activity of mTORC1 and mTORC2 and controls cellular size. *Mol. Cell 42*, 50−61.
(29) Buerger, C., DeVries, B., and Stambolic, V. (2006) Localization of Rheb to the endomembrane is critical for its signaling function. *Biochem. Biophys. Res. Commun. 344*, 869−880.
(30) Bai, X., Ma, D., Liu, A., Shen, X., Wang, Q. J., Liu, Y., and Jiang, Y. (2007) Rheb activates mTOR by antagonizing its endogenous inhibitor, FKBP38. *Science 318*, 977−980.
(31) Fang, Y., Vilella-Bach, M., Bachmann, R., Flanigan, A., and Chen, J. (2001) Phosphatidic acid-mediated mitogenic activation of mTOR signaling. *Science 294*, 1942−1945.
(32) Selvy, P. E., Lavieri, R. R., Lindsley, C. W., and Brown, H. A. (2011) Phospholipase D: Enzymology, functionality, and chemical modulation. *Chem. Rev. 111*, 6064−6119.
(33) Ha, S. H., Kim, D. H., Kim, I. S., Kim, J. H., Lee, M. N., Lee, H. J., Kim, J. H., Jang, S. K., Suh, P. G., and Ryu, S. H. (2006) PLD2 forms a functional complex with mTOR/raptor to transduce mitogenic signals. *Cell. Signalling 18*, 2283−2291.
(34) Foster, D. A. (2009) Phosphatidic acid signaling to mTOR: Signals for the survival of human cancer cells. *Biochim. Biophys. Acta 1791*, 949−955.
(35) Sun, Y., Fang, Y., Yoon, M. S., Zhang, C., Roccio, M., Zwartkruis, F. J., Armstrong, M., Brown, H. A., and Chen, J. (2008) Phospholipase D1 is an effector of Rheb in the mTOR pathway. *Proc. Natl. Acad. Sci. U.S.A. 105*, 8286−8291.
(36) Zhang, C., Wendel, A. A., Keogh, M. R., Harris, T. E., Chen, J., and Coleman, R. A. (2012) Glycerolipid signals alter mTOR complex 2 (mTORC2) to diminish insulin signaling. *Proc. Natl. Acad. Sci. U.S.A. 109*, 1667−1672.
(37) Toschi, A., Lee, E., Xu, L., Garcia, A., Gadir, N., and Foster, D. A. (2009) Regulation of mTORC1 and mTORC2 complex assembly by phosphatidic acid: Competition with rapamycin. *Mol. Cell. Biol. 29*, 1411−1420.
(38) Veverka, V., Crabbe, T., Bird, I., Lennie, G., Muskett, F. W., Taylor, R. J., and Carr, M. D. (2007) Structural characterization of the interaction of mTOR with phosphatidic acid and a novel class of inhibitor: Compelling evidence for a central role of the FRB domain in small molecule-mediated regulation of mTOR. *Oncogene 27*, 585−595.
(39) Dames, S. A. (2008) A fast and simple method to prepare the FKBP-rapamycin binding domain of human target of rapamycin for NMR binding assays. *Protein Expression Purif. 59*, 31−37.
(40) Schanda, P., Kupce, E., and Brutscher, B. (2005) SOFAST-HMQC experiments for recording two-dimensional heteronuclear correlation spectra of proteins within a few seconds. *J. Biomol. NMR 33*, 199−211.
(41) Delaglio, F., Grzesiek, S., Vuister, G. W., Zhu, G., Pfeifer, J., and Bax, A. (1995) NMRPipe: A multidimensional spectral processing system based on UNIX pipes. *J. Biomol. NMR 6*, 277−293.
(42) Johnson, B. A. (2004) Using NMRView to visualize and analyze the NMR spectra of macromolecules. *Methods Mol. Biol. 278*, 313−352.
(43) Veverka, V., Lennie, G., Crabbe, T., Bird, I., Taylor, R. J., and Carr, M. D. (2006) NMR assignment of the mTOR domain responsible for rapamycin binding. *J. Biomol. NMR 36* (Suppl. 1), 3.
(44) Stafford, R. E., Fanni, T., and Dennis, E. A. (1989) Interfacial properties and critical micelle concentration of lysophospholipids. *Biochemistry 28*, 5113−5120.
(45) Kutateladze, T. G., Capelluto, D. G., Ferguson, C. G., Cheever, M. L., Kutateladze, A. G., Prestwich, G. D., and Overduin, M. (2004) Multivalent mechanism of membrane insertion by the FYVE domain. *J. Biol. Chem. 279*, 3050−3057.
(46) Ahn, H. C., Juranic, N., Macura, S., and Markley, J. L. (2006) Three-dimensional structure of the water-insoluble protein crambin in dodecylphosphocholine micelles and its minimal solvent-exposed surface. *J. Am. Chem. Soc. 128*, 4398−4404.
(47) Losonczi, J. A., Olejniczak, E. T., Betz, S. F., Harlan, J. E., Mack, J., and Fesik, S. W. (2000) NMR studies of the anti-apoptotic protein Bcl-xL in micelles. *Biochemistry 39*, 11024−11033.
(48) Dames, S. A., Junemann, A., Sass, H. J., Schonichen, A., Stopschinski, B. E., Grzesiek, S., Faix, J., and Geyer, M. (2011) Structure, dynamics, lipid binding, and physiological relevance of the putative GTPase-binding domain of *Dictyostelium* formin C. *J. Biol. Chem. 286*, 36907−36920.
(49) Weschayanwiwat, P., Scamehorn, J., and Reilly, P. (2005) Surfactant properties of low molecular weight phospholipids. *J. Surfactants Deterg. 8*, 65−72.
(50) Tausk, R. J., Karmiggelt, J., Oudshoorn, C., and Overbeek, J. T. (1974) Physical chemical studies of short-chain lecithin homologues. I. Influence of the chain length of the fatty acid ester and of electrolytes on the critical micelle concentration. *Biophys. Chem. 1*, 175−183.
(51) Hauser, H. (2000) Short-chain phospholipids as detergents. *Biochim. Biophys. Acta 1508*, 164−181.
(52) Odagaki, Y., and Clardy, J. (1997) Structural basis for peptidomimicry by the effector element of rapamycin. *J. Am. Chem. Soc. 119*, 10253−10254.
(53) Choi, J., Chen, J., Schreiber, S. L., and Clardy, J. (1996) Structure of the FKBP12-rapamycin complex interacting with the binding domain of human FRAP. *Science 273*, 239−242.
(54) Moravcevic, K., Oxley, C. L., and Lemmon, M. A. (2012) Conditional Peripheral Membrane Proteins: Facing up to Limited Specificity. *Structure 20*, 15−27.
(55) Banaszynski, L. A., Liu, C. W., and Wandless, T. J. (2005) Characterization of the FKBP·rapamycin·FRB ternary complex. *J. Am. Chem. Soc. 127*, 4715−4721.
(56) Bhat, V., McDonald, C. B., Mikles, D. C., Deegan, B. J., Seldeen, K. L., Bates, M. L., and Farooq, A. (2012) Ligand Binding and Membrane Insertion Compete with Oligomerization of the BclXL Apoptotic Repressor. *J. Mol. Biol. 416*, 57−77.
(57) Bogner, C., Leber, B., and Andrews, D. W. (2010) Apoptosis: Embedded in membranes. *Curr. Opin. Cell Biol. 22*, 845−851.
(58) Yeung, T., Ozdamar, B., Paroutis, P., and Grinstein, S. (2006) Lipid metabolism and dynamics during phagocytosis. *Curr. Opin. Cell Biol. 18*, 429−437.
(59) Xian, W., and Janmey, P. A. (2002) Dissecting the gelsolin-polyphosphoinositide interaction and engineering of a polyphosphoinositide-sensitive gelsolin C-terminal half protein. *J. Mol. Biol. 322*, 755−771.

(60) McMahon, L. P., Choi, K. M., Lin, T. A., Abraham, R. T., and Lawrence, J. C., Jr. (2002) The rapamycin-binding domain governs substrate selectivity by the mammalian target of rapamycin. *Mol. Cell. Biol. 22*, 7428−7438.
(61) Frias, M. A., Thoreen, C. C., Jaffe, J. D., Schroder, W., Sculley, T., Carr, S. A., and Sabatini, D. M. (2006) mSin1 is necessary for Akt/PKB phosphorylation, and its isoforms define three distinct mTORC2s. *Curr. Biol. 16*, 1865−1870.
(62) Zimmerberg, J., and Kozlov, M. M. (2006) How proteins produce cellular membrane curvature. *Nat. Rev. Mol. Cell Biol. 7*, 9−19.
(63) Kam, Y., and Exton, J. H. (2004) Role of phospholipase D1 in the regulation of mTOR activity by lysophosphatidic acid. *FASEB J. 18*, 311−319.
(64) Xu, L., Salloum, D., Medlin, P. S., Saqcena, M., Yellen, P., Perrella, B., and Foster, D. A. (2011) Phospholipase D mediates nutrient input to mammalian target of rapamycin complex 1 (mTORC1). *J. Biol. Chem. 286*, 25477−25486.
(65) Young, B. P., Shin, J. J., Orij, R., Chao, J. T., Li, S. C., Guan, X. L., Khong, A., Jan, E., Wenk, M. R., Prinz, W. A., Smits, G. J., and Loewen, C. J. (2010) Phosphatidic acid is a pH biosensor that links membrane biogenesis to metabolism. *Science 329*, 1085−1088.
(66) Dechant, R., Binda, M., Lee, S. S., Pelet, S., Winderickx, J., and Peter, M. (2010) Cytosolic pH is a second messenger for glucose and regulates the PKA pathway through V-ATPase. *EMBO J. 29*, 2515−2526.
(67) Olsson, M. H. M., Søndergaard, C. R., Rostkowski, M., and Jensen, J. H. (2011) PROPKA3: Consistent Treatment of Internal and Surface Residues in Empirical pKa Predictions. *J. Chem. Theory Comput. 7*, 525−537.
(68) Koradi, R., Billeter, M., and Wuthrich, K. (1996) MOLMOL: A program for display and analysis of macromolecular structures. *J. Mol. Graphics 14*, 29−32 , 51−55.